

A new “gold standard”: perturbative triples corrections in unitary coupled cluster theory and prospects for quantum computing*

Zachary W. Windom^{1,2}, Daniel Claudino^{2†}, and Rodney J. Bartlett¹
¹*Quantum Theory Project, University of Florida, Gainesville, FL, 32611, USA*
²*Computational Sciences and Engineering Division,
 Oak Ridge National Laboratory, Oak Ridge, TN, 37831, USA*

A major difficulty in quantum simulation is the adequate treatment of a large collection of entangled particles, synonymous with electron correlation in electronic structure theory, with coupled cluster (CC) theory being the leading framework in dealing with this problem. Augmenting computationally affordable low-rank approximations in CC theory with a perturbative account of higher-rank excitations is a tractable and effective way of accounting for the missing electron correlation in those approximations. This is perhaps best exemplified by the “gold standard” CCSD(T) method, which bolsters the baseline CCSD with effects of triple excitations using considerations from many-body perturbation theory (MBPT). Despite this established success, such a synergy between MBPT and the unitary analog of CC theory (UCC) has not been explored. In this work, we propose a similar approach wherein converged UCCSD amplitudes, which can be obtained on a quantum computer, are leveraged by a classical computer to evaluate energy corrections associated with triple excitations - leading to the UCCSD[T] and UCCSD(T*) methods. The rationale behind these choices is shown to be rigorous by studying the properties of finite-order UCC energy functionals. Although our efforts do not support the addition of the fifth-order contribution as in the (T) correction, comparisons are nevertheless made using a hybrid UCCSD(T) approach. We assess the performance of these approaches on a collection of small molecules, and demonstrate the benefits of harnessing the inherent synergy between MBPT and UCC theories.

The exact solution of the time-independent, non-relativistic Schrödinger equation is the “holy grail” of quantum chemistry, as *ab initio* prediction of several important molecular and materials properties becomes immediately accessible.¹ Unfortunately, full configuration interaction (FCI), i.e., the accounting of all possible electronic configurations in a one-particle basis, scales combinatorially with system size, meaning that the exact solution is beyond reach for the vast majority of chemical space. Nevertheless, methods based on low-rank coupled-cluster (CC) theory have the advantage of converging rapidly to the FCI limit in polynomial time,² and therefore are of immense value to the computational chemistry and materials science communities.³ In fact, systematic convergence to FCI is assured by considering higher-rank cluster operators into the ansätze albeit at increasing computational cost.⁴

Contrary to approaches centered around expectation values, CC lends itself to a series of residual equations emerging from projections of the Schrödinger equation onto the space of excitations out of the reference function, typically Hartree-Fock (HF), but applicable to any single determinant that overlaps with the exact wavefunction. One way to circumnavigate the mounting intractability in including arbitrarily high-orders of the cluster operator is to introduce corrections *post hoc* based on some flavor of perturbation theory. The most prominent of these methods is the perturbative energy correction for triple excitations with infinite-order single (S) and double (D) excitations that results in the CCSD(T) method⁵⁻⁷ - the so-called “gold standard” of quantum chemistry. And, on the same token, a similar philosophy can be used to bolster - for example, CCSDT - by incorporating a perturbative treatment of missed quadruple excitations.⁸ This framework ultimately culminates in a hierarchy of methods whose focus is to provide a perturbative estimate of electron correlation associated with higher-rank cluster operators that are explicitly omitted once the cluster operator has been truncated.⁹ Methods based on the factorization theorem of MBPT have also been proposed and investigated,¹⁰ showing that further reduction in calculation cost can be achieved while simultaneously providing some estimate of higher-order correlation effects.¹¹⁻¹³

A simplistic view of the CC ansatz would define it as an exponential map of excitation operators, which is used in its predominant projective variant. This “simplicity” arises by virtue of the natural truncation of the Baker-Campbell-Hausdorff expansion of the similarity-transformed Hamiltonian, and it comes at the expense of a loss of unitarity/variationality. However, other perspectives have investigated alternative CC ansätze¹⁴ in the pursuit of

† claudinodc@ornl.gov

*This manuscript has been authored by UT-Battelle, LLC, under Contract No. DE-AC0500OR22725 with the U.S. Department of Energy. The United States Government retains and the publisher, by accepting the article for publication, acknowledges that the United States Government retains a non-exclusive, paid-up, irrevocable, world-wide license to publish or reproduce the published form of this manuscript, or allow others to do so, for the United States Government purposes. The Department of Energy will provide public access to these results of federally sponsored research in accordance with the DOE Public Access Plan.

satisfying exact conditions,^{14,15} such as the generalized Hellman-Feynman (GHF) theorem.¹⁶ The original expectation value formalism¹⁷ - which, in the limit, converges toward variational CC^{18,19} - and the unitary CC (UCC) ansätze²⁰ fall into this category. By design, these ansätze are arguably more suitable for the calculation of properties as compared to the standard CC formulation. Unfortunately, they inherently scale as FCI since the Hamiltonian-cluster commutator expansion does not truncate.⁴ Again, perturbation theory can be used to “pick” a suitable truncation point for tractability,²¹ although admittedly methods that are truncated at low-orders do not necessarily provide results that are comparable to similar, standard CC counterparts.^{22,23} Alternatively, truncations based on commutator-rank have also been explored.^{24,25}

This impasse between projective and alternative ansätze may potentially be solved with the emergence of quantum computing paradigms, which would enable UCC without resorting to arbitrary truncation. This is because the UCC ansätze can be effectively encoded as a series of gate-based operations acting on an *easy-to-prepare* state,^{26,27} e.g. HF. In fact, there is supporting evidence that untruncated UCC theory provides more accurate results than the equivalent, standard CC method.¹⁹ Nevertheless, fundamental issues inhibit routine UCC calculations on a quantum computer; notably, circuit width and depth – either of which ultimately restrict the maximal rank of the cluster operator.²⁸ This is clearly unfortunate since it is known that the only way CC/UCC converges toward the exact solution of the Schrödinger equation (in a basis set) is by adding the abovementioned higher-rank cluster operators. A further point of consideration lies in the distinction between the complete, non-terminating UCC ansatz and the Trotterized, or so-called *disentangled*, counterpart, with the latter rising from known product formulas and proven exact under certain conditions.²⁹

To address the lack of a framework enabling perturbative corrections for the UCC ansatz, we explore potential synergies between MBPT and UCC theory which have not been scrutinized until now. By studying the properties of finite-order UCC equations, we propose a pathway towards perturbative corrections to the infinite-order UCCSD energy designed to recover the missed effects of higher-rank excitations, which we illustrate by introducing the UCCSD[T] and UCCSD(T*) methods, unitary analogs of the pioneering perturbative accounting for triple excitations.⁵ We show that such an approach is a robust way of recovering electron correlation that is missed by restricting the unitary cluster operator. By employing what can be seen as a post-processing step born from rigorous theory, our results reinforce the perspective that resource-efficient interplay between quantum and classical computers should be harnessed to achieve more accurate results without imposing extra burden on current, fragile quantum computers.

We motivate the problem using semi-canonicalized orbitals for a general reference function, e.g., non-HF. The normal-ordered Hamiltonian is then of the form

$$H_N = \underbrace{\left(\sum_p \epsilon_{pp} \{p^\dagger p\} \right)}_{f_N} + \underbrace{\left(\sum_{ia} f_{ia} \{i^\dagger a\} + \sum_{ai} f_{ai} \{a^\dagger i\} + \frac{1}{4} \sum_{pqrs} \langle pq || rs \rangle \{p^\dagger q^\dagger sr\} \right)}_{W_N}, \quad (1)$$

where indices $a, b, c, d \dots, i, j, k, l \dots$, and $p, q, r, s \dots$ specify virtual, occupied, and arbitrary spin-orbitals. Note that the perturbation W_N now contains the occupied/virtual blocks of the Fock operator.

Standard CC theory begins by defining the form of the cluster operator, T ,

$$T = T_1 + T_2 + T_3 + \dots, \quad (2)$$

where each T_n can be expressed in the language of second quantization as

$$T_n = \frac{1}{(n!)^2} \sum_{\substack{a,b,c,\dots \\ i,j,k,\dots}} t_{ijk\dots}^{abc\dots} \{a^\dagger i b^\dagger j c^\dagger k \dots\}. \quad (3)$$

Once an appropriate level of cluster restriction has been chosen, the unitary cluster operator can be defined as

$$\tau = T - T^\dagger, \quad (4)$$

where our working assumption is that we are using real orbitals, hence $t_{ij\dots}^{ab\dots*} = t_{ij\dots}^{ab\dots}$. In this context, the Schrödinger equation becomes

$$H_N e^\tau |0\rangle = (H_N e^\tau)_C |0\rangle = \Delta E e^\tau |0\rangle, \quad (5)$$

with C indicating a restriction to connected diagrams and $\Delta E = E_{CC} - E_{HF}$ being the correlation energy. We point out that if we follow the traditional CC route of projecting Equation 5 onto elements of the excitation manifold, the resulting residual equations will not terminate. Therefore, we have to pick a point to truncate the resulting expressions based on some specified criteria. Unlike prior work on the topic,^{20,30} we define orders in terms of W_N assuming a

non-canonical HF reference, denoted by $|0\rangle$. In other words, f_N is zeroth-order and W_N arises in first-order of MBPT and therefore both τ_1 and τ_2 show up at first-order whereas the remaining higher-order operators, τ_n , arise in the $(n-1)$ -order wavefunction of MBPT.

For the purposes of this work, our starting point is the complete, fourth-order UCC(4) energy functional

$$\begin{aligned}
\Delta E(4) = & -\langle 0 | \frac{1}{3!} \left((T_1^\dagger)^2 T_1 f_N T_1 + \text{h.c.} + (T_2^\dagger)^2 T_2 f_N T_2 + \text{h.c.} \right) + \frac{1}{2} \left(T_3^\dagger T_1 f_N T_2 + \text{h.c.} + T_3^\dagger T_2 f_N T_1 + \text{h.c.} \right) |0\rangle \\
& - \frac{1}{3} \langle 0 | T_1^\dagger T_2^\dagger T_1 f_N T_2 + \text{h.c.} + T_2^\dagger T_1^\dagger T_2 f_N T_1 + \text{h.c.} |0\rangle \\
& - \langle 0 | \frac{1}{3!} \left((T_1^\dagger)^2 T_1 W_N + \text{h.c.} \right) + \frac{1}{3!} \left((T_2^\dagger)^2 T_2 W_N + \text{h.c.} \right) + \frac{1}{2} \left(T_3^\dagger T_1 W_N + \text{h.c.} + T_3^\dagger T_2 W_N + \text{h.c.} \right) |0\rangle \\
& - \frac{1}{3} \langle 0 | T_1^\dagger T_2^\dagger T_1 W_N + \text{h.c.} + T_2^\dagger T_1^\dagger T_2 W_N + \text{h.c.} |0\rangle - \frac{1}{6} \langle 0 | T_2^\dagger T_1 T_1^\dagger f_N T_2 + \text{h.c.} + T_2^\dagger T_1 T_1^\dagger W_N + \text{h.c.} |0\rangle \\
& + \frac{1}{4} \langle 0 | (T_1^\dagger)^2 f_N T_1^2 + (T_2^\dagger)^2 f_N T_2^2 |0\rangle + \langle 0 | T_3^\dagger f_N T_3 |0\rangle + \langle 0 | T_3^\dagger f_N T_1 T_2 + \text{h.c.} |0\rangle + \langle 0 | T_1^\dagger T_2^\dagger f_N T_1 T_2 |0\rangle \\
& + \frac{1}{2} \langle 0 | (T_1^\dagger)^2 W_N T_1 + \text{h.c.} + (T_2^\dagger)^2 W_N T_2 + \text{h.c.} |0\rangle + \langle 0 | T_3^\dagger W_N (T_1 + T_2) + \text{h.c.} |0\rangle + \langle 0 | T_2^\dagger T_1^\dagger W_N (T_1 + T_2) + \text{h.c.} |0\rangle \\
& - \frac{1}{2} \langle 0 | T_2^\dagger T_1 W_N (T_1 + T_2) + \text{h.c.} |0\rangle + \frac{1}{2} \langle 0 | (T_1^\dagger)^2 W_N T_2 + \text{h.c.} |0\rangle.
\end{aligned} \tag{6}$$

Although Equation 6 involves fully linked diagrams that are connected overall, there may be instances where the underlying diagram is internally disconnected and therefore requires cancellation. The Supplementary Material discusses how to resolve such examples, and also provides the complete derivations for UCC(2), UCC(3), and UCC(4) in the case of non-canonical HF orbitals.

With this in mind, several internal cancellations are found in Equation 6, leading to a simplified expression for the UCC(4) functional. From there, the residual equations can be formulated:

$$\frac{\partial \Delta E(4)}{\partial T_1^\dagger} = 0 \Rightarrow D_1 T_1 = W_N + W_N T_2 + W_N T_1 + \frac{1}{2} \left(\frac{1}{2} W_N T_1^2 + T_1^\dagger W_N T_1 \right) + T_2^\dagger W_N T_2, \tag{7a}$$

$$\frac{\partial \Delta E(4)}{\partial T_2^\dagger} = 0 \Rightarrow D_2 T_2 = W_N + W_N T_2 + W_N T_1 + \frac{1}{2} \left(\frac{1}{2} W_N T_2^2 + T_2^\dagger W_N T_2 \right) + W_N T_3 + T_1^\dagger W_N T_2 + W_N T_1 T_2, \tag{7b}$$

$$\frac{\partial \Delta E(4)}{\partial T_3^\dagger} = 0 \Rightarrow D_3 T_3 = W_N T_2. \tag{7c}$$

After inserting these stationary conditions into the simplified form of Equation 6, the final, reduced UCC(4) energy is shown to be

$$\Delta E(4) = \langle 0 | W_N T_2 |0\rangle + \langle 0 | W_N T_1 |0\rangle - \frac{1}{4} \left(\langle 0 | (T_1^\dagger)^2 W_N T_1 |0\rangle + \langle 0 | (T_2^\dagger)^2 W_N T_2 |0\rangle \right). \tag{8}$$

The following developments focus on Equations 7 and 8 where we are only interested in fully iterating the singles/doubles equations. In order to derive perturbative corrections designed to account for missing T_3 -like excitations in UCCSD-like methods, we “trace” the residual equations - starting with the T_3 equation of Equation 7 - to determine this operator’s role in the UCC(4) energy. As the derived UCC(4) equations are subsumed within those of UCC($n \rightarrow \infty$), any set of T_3 corrections designed for UCCSD(4) are equally viable for infinite-order UCCSD.

This procedure starts by circumnavigating the explicit solution for the T_3 equations by adopting the approximation

$$T_3^{[2]} = \frac{1}{D_3} (W_N T_2)_C \tag{9}$$

using T_2 amplitudes from any converged, UCCSD-like calculation. The superscript denotes the order in MBPT through which this contribution is correct, meaning that in this case, $T_3^{[2]}$ is correct through second-order in MBPT. Although T_3 is not directly specified in Equation 8, it does couple to the T_2 equation. Inserting Equation 9 into 7b, we find that

$$T_2^{[3]} \equiv \frac{1}{D_2} (W_N T_3^{[2]} + f_{ia} T_3^{[2]})_C, \tag{10}$$

Note that these contributions are “new” in the sense that they originate from an approximate solution to T_3 . By inserting this “new” $T_2^{[3]}$ into the first term of Equation 8, we can recover a correction to either UCCSD(4) and/or the infinite-order UCCSD energy which solely originates from $T_3^{[2]}$

$$\begin{aligned} \Delta E(T_3^{[2]}) &= \langle 0 | W_N T_2^{[3]} | 0 \rangle \\ &\approx \langle 0 | T_2^\dagger \left(W_N T_3^{[2]} + f_{ia} T_3^{[2]} \right)_C | 0 \rangle. \end{aligned} \quad (11)$$

Note that the standard convention is to cap with an infinite-order T_2^\dagger , shown in the final line of Equation 11. These two terms ultimately lead to diagrams C and D in Figure 1, where diagram C in particular defines the [T] correction⁵ and the combination of diagrams C, D, and F account for the standard (T) correction for non-canonical orbitals.

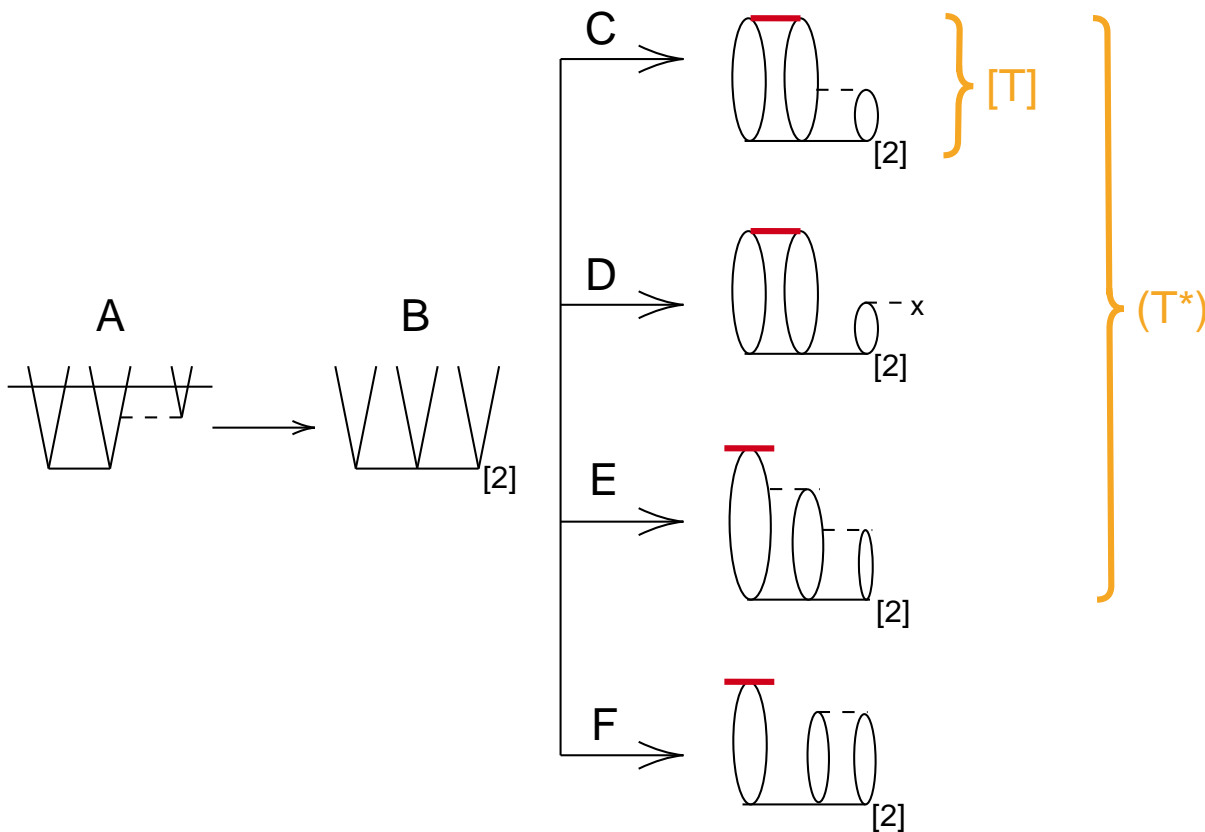


FIG. 1: Outline of the procedure to extract triples’ energy corrections by A) approximating T_3 with $(W_N T_2)_C$, B) we now have a T_3 correct through second-order in MBPT. If the UCC(4) equations are traced, diagram C) - which completely defines the [T] correction - and D) are rigorously shown to originate at fourth-order in MBPT. These diagrams, along with diagram E) - which represents a fifth-order contribution in MBPT - define the (T*) method. The standard (T) formulation, which is composed of diagrams C), D) and F), is also studied in this work, despite the fact that diagram F) does not exist in UCC(4).

The remaining diagram in (T) takes the form $\langle 0 | T_1^\dagger W_N T_3^{[2]} | 0 \rangle$ and appears as F in Figure 1. As shown in the Supplementary Material, this term is completely canceled in the UCC(4) functional. Consequently, this diagram is not rigorously achievable by beginning with T_3 and tracing the residual equations.

However, a similar term of the form $Q_1 (T_2^\dagger (W_N T_2)_C)$ does exist in the UCC(4) T_1 equation, where the subtle relationship with the T_3 equations is noted and Q_1 is the projector onto single excitations. Inserting this term directly into the UCC(4) energy expression gives rise to a diagram that is strikingly similar to diagram F, but which is

independent of the set of triples excitations that are directly tied to the T_3 operator; this can be seen by the absence of any factors of $\frac{1}{D_3}$. Despite yielding a net excitation effect that *appears* as triples, the overall diagram is managed solely by products of T_1 , T_2 , and W_N making its contribution redundant for our purposes.

We can nevertheless search for a similar diagram that caps with a T_1^\dagger , by tracing the logic followed by the [T] developments. Assuming we are interested in only low-order contributions, we can start by solving the T_3 residual equations of Equation 7 for second-order T_3 :

$$T_3^{[2]} = \frac{1}{D_3}(W_N T_2)_C, \quad (12)$$

then plug Equation 12 to determine a contribution to Equation 7b:

$$T_2^{[3]} = \frac{1}{D_2} \left(W_N \left(\frac{1}{D_3} (W_N T_2)_C \right) \right)_C, \quad (13)$$

which in turn couples to 7a:

$$T_1^{[4]} = \frac{1}{D_1} \left(W_N \frac{1}{D_2} \left(W_N \left(\frac{1}{D_3} (W_N T_2)_C \right) \right)_C \right)_C, \quad (14)$$

and finally, we insert Equation 14 into Equation 8 to determine what amounts to a fifth-order correction to the energy that also originates from T_3

$$\begin{aligned} \Delta E(T_1^{[4]}) &= \langle 0 | W_N T_1^{[4]} | 0 \rangle \\ &\approx \langle 0 | T_1^\dagger \left(W_N \frac{1}{D_2} \left(W_N \left(\frac{1}{D_3} (W_N T_2)_C \right) \right)_C \right)_C | 0 \rangle, \end{aligned} \quad (15)$$

The combination of the last line of Equation 15 - depicted in Figure 1 E - and Equation 11 leads to a new method referred to as (T*).

As before, we choose to cap with an infinite-order T_1^\dagger in Equation 15 instead of $T_1^{[1]\dagger}$ to define the correction.

The following UCC results are obtained using the XACC quantum computing framework,³¹ and PySCF³² to generate the Hamiltonians, to calculate FCI energies, and to select important τ 's suggested by CCSD amplitudes. Converged UCC amplitudes are then manipulated by the UT2 python module to extract the triples corrections. Standard CC calculations were performed using CFOUR³³ and ACESII³⁴. The STO-6G³⁵ basis set was used throughout this work, and core orbitals were dropped, with details regarding the electronic state and geometries being provided in Table S1 of the Supplementary Material.

All FCI, UCCSD, UCCSD[T], and UCCSD(T*) energies are provided in Table S2 of the Supplementary Material. Despite the lack of a rigorous basis, we also provide results using the (T) correction - denoted as UCCSD(T).

With quantum computing in the background, two forms of UCC ansatz are adopted here. The first follows closely the standard CC formalism where we simply replace the routine T cluster operator by its anti-Hermitian analog τ and construct the exponential wave operator:

$$|\Psi_{\text{UCCSD}}\rangle = e^{\sum_{ia} \theta_i^a (a^\dagger i - \text{h.c.}) + \sum_{ijab} \theta_{ij}^{ab} (a^\dagger b^\dagger ij - \text{h.c.})} |0\rangle. \quad (16)$$

As previously noted, this ansatz does not naturally truncate the underlying Schrödinger equation as does the standard T . A form of this operator more suitable for implementation on a quantum computer is the Trotterized or disentangled form of the ansatz, which we refer to as tUCCSD hereafter

$$|\Psi_{\text{tUCCSD}}\rangle = \prod_{IA} e^{\theta_I^A (A^\dagger I - \text{h.c.})} e^{\theta_{\bar{I}}^{\bar{A}} (\bar{A}^\dagger \bar{I} - \text{h.c.})} \prod_{\substack{I < J \\ A < B}} e^{\theta_{IJ}^{AB} (A^\dagger B^\dagger IJ - \text{h.c.})} e^{\theta_{\bar{I}\bar{J}}^{\bar{A}\bar{B}} (\bar{A}^\dagger \bar{B}^\dagger \bar{I}\bar{J} - \text{h.c.})} \prod_{IJAB} e^{\theta_{IJ}^{AB} (A^\dagger B^\dagger IJ - \text{h.c.})} |0\rangle, \quad (17)$$

with I, J, A, B indexing α orbitals and $\bar{I}, \bar{J}, \bar{A}, \bar{B}$ indexing the corresponding β orbitals.

While the UCCSD ansatz in Equation 16 is unique, the composition of the excitation operators alone will not uniquely define its Trotterized analog, since such operators do not commute in general. The potential ambiguity is removed by fully specifying the indices over the products in Equation 17. Such ordering is in line with previous results. However, it is not adequate for geometries away from equilibrium, as will be discussed later.³⁶ As shown later on, the energy difference between UCCSD and tUCCSD - as well as the corresponding triples corrections - is nominal.

In this work we analyze the performance of three classes of CC/UCC methods:

1. “Standard” CC methods that incorporate triples corrections into CCSD, namely CCSD[T], CCSD(T), CCSDT-1, and ACCSD(T);
2. Truncated UCC methods through fourth-order;
3. Infinite-order UCCSD and tUCCSD - and the corresponding [T], (T*), and (T) corrections.

The main goal of this paper is to evaluate the performance of methods under class 3, that is, UCCSD[T]/(T)/(T*) and tUCCSD[T]/(T)/(T*). Those are built with the set of optimal τ_1 and τ_2 learned by subjecting the two choices of ansätze to the Variational Quantum Eigensolver algorithm (VQE)³⁷

$$\tau_1^*, \tau_2^* = \arg \min_{\tau_1, \tau_2} \langle \Psi(\tau_1, \tau_2) | H | \Psi(\tau_1, \tau_2) \rangle, \quad (18)$$

with τ_1^* and τ_2^* being employed in the diagrams in Figure 1 and Equations 11-15.

Table I records the error of each method against FCI, which is found in the range of 50-271 mH, and the corresponding percentage of total correlation energy. “Standard” CC methods largely align with FCI, with CCSD missing up to 16 mH of correlation energy in the worst case. The inclusion of (T) represents a significant improvement, where we close the diagram of Figure 1 with a converged T_2^\dagger amplitude. We note that T_2^\dagger is the lowest-order approximation to the complete solution of the left-hand eigenvalue problem defining Λ_2 .³⁸ If we, instead, cap the diagram of Figure 1 using Λ_2 - resulting in Λ CCSD(T) - the results are slightly worse than CCSD(T), except for CO. This is somewhat counter-intuitive, but is a trend that has already been previously observed.³⁹ Overall, the infinite-order CCSDT-1 shows the best performance amongst the methods we consider. It takes the T_2 portion of the diagram in Figure 1 and adds it to the CCSD T_2 residual equations, accounting for some coupling between T_2 and a diagram that originates from T_3 at lowest order. Thus, the energy “feels” effects from this diagram that originate from $T_3^{[2]}$, and is responsible for this improvement.

TABLE I: Error with respect to FCI, in mH, and the corresponding percentage of the total correlation energy (in parentheses). ‡ denotes an all electron calculation.

Method	H ₂ O	CO	C ₂	O ₂	N ₂
UCCSD	-0.100 (99.79)	-8.183 (94.12)	-11.90 (95.61)	-9.132 (94.15)	-2.176 (98.62)
UCCSD[T]	-0.023 (99.95)	-6.105 (95.61)	4.841 (101.78)	-6.018 (96.14)	-0.383 (99.75)
UCCSD(T)	-0.015 (99.97)	-5.973 (95.71)	8.247 (103.04)	-5.979 (96.17)	-0.356 (99.78)
UCCSD(T*)	-0.023 (99.95)	-6.071 (95.64)	7.004 (102.58)	-6.002 (96.16)	-0.371 (99.77)
tUCCSD	-0.098 (99.80)	-7.888 (94.33)	-11.08 (95.91)	-9.122 (94.16)	-2.172 (98.62)
tUCCSD[T]	-0.020 (99.95)	1.776 (101.27)	6.109 (102.25)	-5.842 (96.25)	-0.623 (99.60)
tUCCSD(T)	-0.012 (99.98)	3.021(102.17)	9.967 (103.67)	-5.801 (96.29)	-0.597 (99.62)
tUCCSD(T*)	-0.021 (99.96)	2.147 (101.54)	8.565 (103.16)	-5.826 (96.27)	-0.612 (99.61)
CCSD	-0.118 (99.76)	-8.157 (94.14)	-16.33 (93.98)	-10.47 (93.29)	-3.983 (97.48)
CCSD(T)	-0.050 (99.89)	-0.865 (99.37)	-2.817 (98.96)	-7.411 (95.25)	-2.231 (98.59)
CCSDT-1	-0.048 (99.9)	1.163 (100.83)	-2.774 (98.97)	-6.201 (96.02)	-2.164 (98.63)
Λ CCSD(T)	-0.085 (99.82)	0.574 (100.41)	-4.375 (98.38)	-7.819 (94.99)	-2.294 (98.55)
UCC(2)	-14.22 (71.56)	-10.74 (92.28)	-25.29 (90.68)	-29.76 (80.94)	-2.921 (98.15)
UCC(3)	0.338 (100.67)	-9.795 (92.96)	-14.97 (94.48)	-2.312 (98.51)	-1.036 (99.34)
UCC(4) [‡]	0.942 (101.88)	9.555 (106.84)	31.46 (111.56)	-21.77 (88.81)	1.707 (101.07)
UCCSD(4) [‡]	0.858 (101.71)	2.326 (98.33)	6.288 (102.31)	-31.61 (83.75)	-0.346 (99.78)
UCCSD(4)[T] [‡]	0.936 (101.87)	7.697 (105.51)	19.81 (107.28)	-29.77 (84.7)	1.396 (100.87)

Moving to the truncated UCC methods, we see that UCC(2) - or equivalently MBPT(2) - captures 71-98% of the correlation energy across the set of molecules tested, and is consistently above FCI by 3-30 mH. UCC(3) - or equivalently LCCD - is a marked improvement, reporting errors no larger than 15 mH. The results from UCC(4) are less straightforward; except in the case of CO, UCC(3) results are in overall better agreement with FCI. We also note that - except in the case of the ¹ Δ state of O₂ - UCC(4) consistently underestimates FCI. A byproduct of prematurely terminating the commutator expansion is that we forgo any guarantee of achieving an upper bound to FCI, as might otherwise be realized by a fully variational method. Noting the exception of O₂ again, we find that omitting the triples portion of UCC(4) - which defines the UCCSD(4) method - has been shown to lead to improvements,²² and is

of comparable quality to UCC(3). By adding the [T] correction for the missed triple excitations on top of UCCSD(4), the resulting UCCSD(4)[T] method - with the exception being O_2 - seems to represent a middle ground between UCCSD(4) and UCC(4). This indicates that adding perturbative triples corrections is a step toward the complete UCC(4) method which iterates the triples residual equations.

Turning to the infinite-order UCC methods, both the UCCSD and tUCCSD methods are of comparable or superior quality to the standard CCSD method, and in either representation of UCCSD adding [T] yields a clear and consistent improvement over the baseline ansätze. In fact, for H_2O , C_2 , and N_2 the [T] variants of UCCSD are within 1% of the FCI. For O_2 , adding [T] nevertheless improves upon the t/UCCSD energy by 2%. This is also true for CO when using UCCSD[T], but for this case the tUCCSD[T] result recovers 6% to the tUCCSD correlation energy. By adding the (T) and (T*) diagrams, we do not find appreciable performance gains over baseline [T]. In fact, for C_2 both t/UCCSD[T] models are noticeably better than their alternative triples counterparts.

A visual comparison of these infinite-order UCC methods and their “standard” CC counterparts is shown in Figure 2. Here, we see that the UCC-based [T] offers the best performance for both N_2 and O_2 , whereas the standard CC (T) correction yields better results for CO and C_2 .

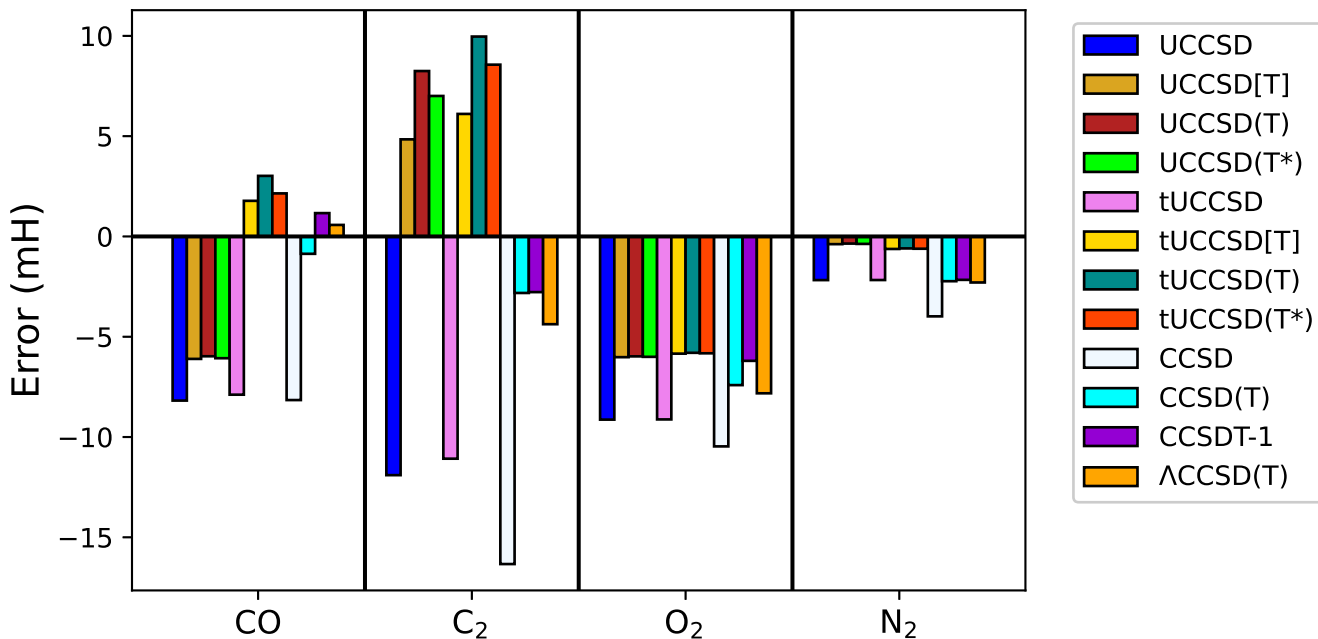


FIG. 2: Bar plot of the errors reported in Table I

Outside the equilibrium region, the [T] correction to UCCSD yields more dramatic improvements as compared to the standard CCSD and CCSD(T) methods. This is illustrated in Figure 3 which show the potential energy surface (PES) of N_2 . Around 1.75 Å, standard CCSD/CCSD(T) methods begin to display the typical drastic divergence from FCI. However, both variants of UCCSD[T] results are better-behaved in this regime.

Beyond 2.2 Å, tUCCSD[T] exhibits perplexing behavior that is not seen in UCCSD[T], as shown in Figure S1 of the Supplementary Material. It is known that one byproduct of the tUCCSD ansatz is the inherent sensitivity to operator ordering.³⁶ While both UCCSD and tUCCSD ansätze remain variational upper bounds to FCI - as expected - it is intriguing that only the [T] corrections built upon tUCCSD behave poorly in this region. Further analysis of the role of the operator ordering is deferred to the Supplementary Material.

In summary, we study finite-orders of UCC theory to design a perturbative treatment for triple excitations in infinite-order UCCSD, in line with what gave rise to the so-called “gold standard” of quantum chemistry. We show that such an approach reliably improves the energy of several small molecules at - or near - equilibrium geometries as compared to baseline UCCSD. This result is independent of whether the full or Trotterized UCCSD operator is used. We find that the differences between the (T) and (T*) approaches are largely indistinguishable, and do not represent significant improvements over the [T] results. An important finding is that the corrections presented here are much more resilient to the typical breakdown characteristic of methods based on perturbation theory when we go beyond the Coulson-Fischer point, in this case for N_2 , despite the tUCCSD-based corrections eventually displaying erroneous behavior which can be attributed to the operator ordering in the tUCCSD ansätze.

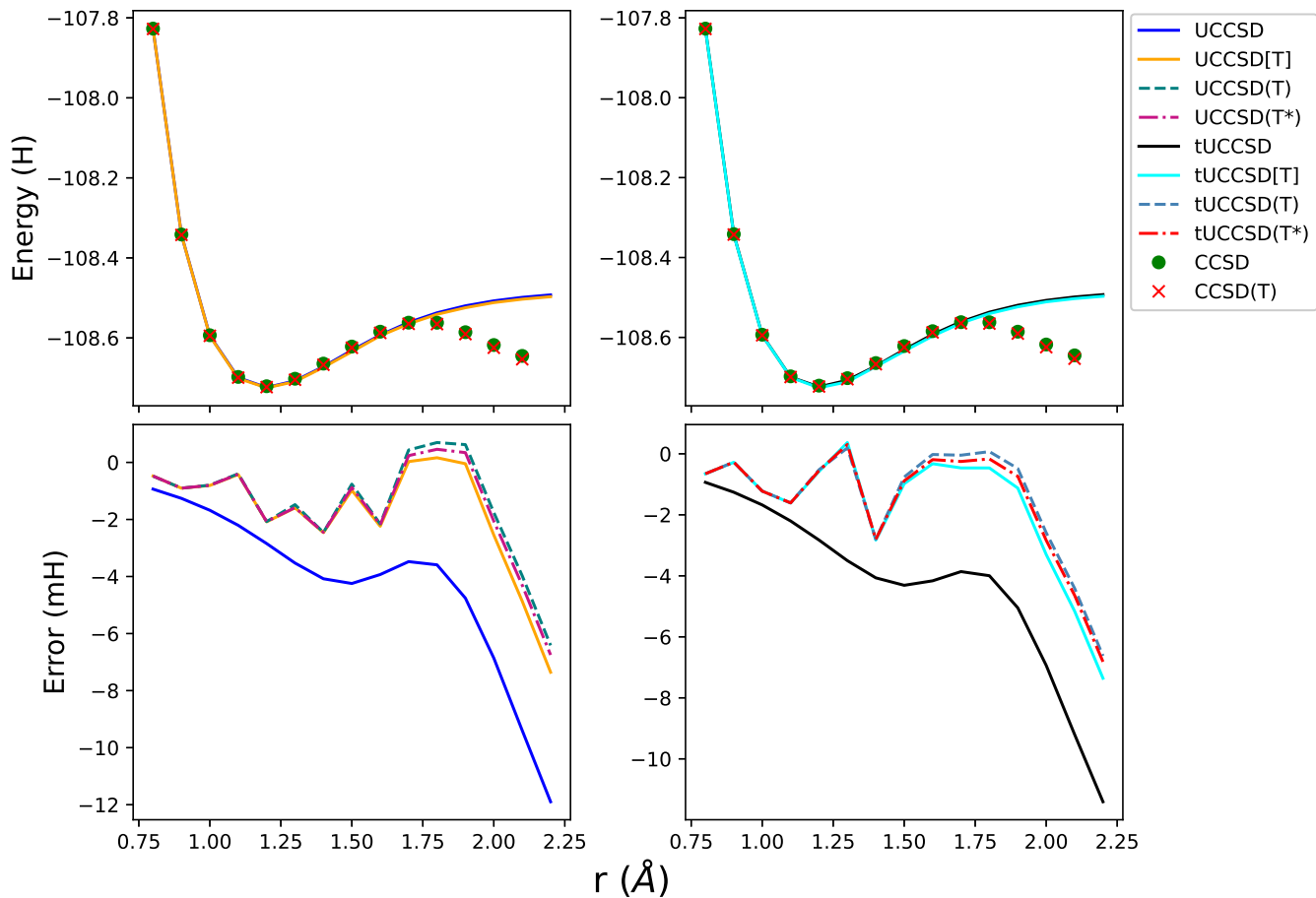


FIG. 3: Comparison of the UCCSD/[T]/(T)/(T*) and tUCCSD/[T]/(T)/(T*) results for the dissociation of N_2 .

The current work opens the door to several topics worth exploring. The most immediate is that it naturally lends itself to the development of additional perturbative corrections. For example, it is conceivable that energy corrections originating from T_1 could be constructed to account for missing single excitation effects in infinite-order t/UCCD by studying the UCC(4) equations for T_1 and tracing the logic followed in the development of UCCSD[T]. In addition to the inherent formal contribution of MBPT in conjunction with the UCC ansatz, the ideas presented here have potential applications in quantum computing. More specifically, energy corrections become accessible from hybrid algorithms – e.g. VQE – with a classical post-processing step free from requiring extra quantum resources. This is embodied by the evaluation of the diagrams in Figure 1 constructed using τ_1 and τ_2 , which can be obtained on a quantum computer. Continued efforts focusing on the symbiotic relationship between MBPT and UCC that exploit hybrid classical/quantum computing algorithm paradigms will be the target of forthcoming work.

Acknowledgements

D.C. and Z.W.W. thank Karol Kowalski for various fruitful discussions. Z.W.W. also thanks Dr. Taylor Barnes of MolSSI for his guidance in developing the UT2 software. This work was supported by the Air Force Office of Scientific Research under AFOSR Award No. FA9550-23-1-0118. Z.W.W. thanks the National Science Foundation and the Molecular Sciences Software Institute for financial support under Grant No. CHE-2136142. Z.W.W. also acknowledges support from the U.S. Department of Energy, Office of Science, Office of Workforce Development for Teachers and Scientists, Office of Science Graduate Student Research (SCGSR) program. The SCGSR program is administered by the Oak Ridge Institute for Science and Education (ORISE) for the DOE. ORISE is managed by ORAU under contract number DE-SC0014664. D.C. acknowledges support by the “Embedding Quantum Computing into Many-body Frameworks for Strongly Correlated Molecular and Materials Systems” project, which is funded by the U.S. Department of Energy (DOE), Office of Science, Office of Basic Energy Sciences, the Division of Chemical

-
- ¹ Bartlett R J 1989 *The Journal of Physical Chemistry* **93** 1697–1708
 - ² Bartlett R J and Musiał M 2007 *Reviews of Modern Physics* **79** 291
 - ³ Zhang I Y and Grüneis A 2019 *Frontiers in Materials* **6** 123
 - ⁴ Shavitt I and Bartlett R J 2009 *Many-body methods in chemistry and physics: MBPT and coupled-cluster theory* (Cambridge university press)
 - ⁵ Urban M, Noga J, Cole S J and Bartlett R J 1985 *The Journal of Chemical Physics* **83** 4041–4046
 - ⁶ Raghavachari K, Trucks G W, Pople J A and Head-Gordon M 1989 *Chemical Physics Letters* **157** 479–483
 - ⁷ Watts J D, Gauss J and Bartlett R J 1993 *The Journal of Chemical Physics* **98** 8718–8733
 - ⁸ Kucharski S A and Bartlett R J 1989 *Chemical Physics Letters* **158** 550–555
 - ⁹ Bartlett R J, Watts J, Kucharski S and Noga J 1990 *Chemical Physics Letters* **165** 513–522
 - ¹⁰ Kucharski S A and Bartlett R J 1986 Fifth-order many-body perturbation theory and its relationship to various coupled-cluster approaches *Advances in Quantum Chemistry* vol 18 (Elsevier) pp 281–344
 - ¹¹ Kucharski S A and Bartlett R J 1998 *The Journal of Chemical Physics* **108** 9221–9226
 - ¹² Kucharski S A and Bartlett R J 1998 *The Journal of Chemical Physics* **108** 5243–5254
 - ¹³ Kucharski S A and Bartlett R J 1998 *The Journal of Chemical Physics* **108** 5255–5264
 - ¹⁴ Szalay P G, Nooijen M and Bartlett R J 1995 *The Journal of Chemical Physics* **103** 281–298
 - ¹⁵ Bartlett R J, Kucharski S A, Noga J, Watts J D and Trucks G W 1989 Some consideration of alternative ansatz in coupled-cluster theory *Many-Body Methods in Quantum Chemistry: Proceedings of the Symposium, Tel Aviv University 28–30 August 1988* (Springer) pp 125–149
 - ¹⁶ Helgaker T U and Almlöf J 1984 *International Journal of Quantum Chemistry* **26** 275–291
 - ¹⁷ Bartlett R J and Noga J 1988 *Chemical Physics Letters* **150** 29–36
 - ¹⁸ Van Voorhis T and Head-Gordon M 2000 *The Journal of Chemical Physics* **113** 8873–8879
 - ¹⁹ Cooper B and Knowles P J 2010 *The Journal of Chemical Physics* **133**
 - ²⁰ Bartlett R J, Kucharski S A and Noga J 1989 *Chemical Physics Letters* **155** 133–140
 - ²¹ Taube A G and Bartlett R J 2006 *International Journal of Quantum Chemistry* **106** 3393–3401
 - ²² Watts J D, Trucks G W and Bartlett R J 1989 *Chemical Physics Letters* **157** 359–366
 - ²³ Byrd J N, Lotrich V F and Bartlett R J 2014 *The Journal of Chemical Physics* **140**
 - ²⁴ Liu J and Cheng L 2021 *The Journal of Chemical Physics* **155**
 - ²⁵ Liu J, Matthews D A and Cheng L 2022 *Journal of Chemical Theory and Computation* **18** 2281–2291
 - ²⁶ Anand A, Schleich P, Alperin-Lea S, Jensen P W, Sim S, Díaz-Tinoco M, Kottmann J S, Degroote M, Izmaylov A F and Aspuru-Guzik A 2022 *Chemical Society Reviews* **51** 1659–1684
 - ²⁷ Chen J, Cheng H P and Freericks J K 2021 *Journal of Chemical Theory and Computation* **17** 841–847
 - ²⁸ Claudino D 2022 *International Journal of Quantum Chemistry* **122** e26990
 - ²⁹ Evangelista F A, Chan G K and Scuseria G E 2019 *The Journal of Chemical Physics* **151**
 - ³⁰ Kutzelnigg W 1991 *Theoretica Chimica Acta* **80** 349–386 ISSN 1432-2234 URL <http://dx.doi.org/10.1007/BF01117418>
 - ³¹ McCaskey A J, Lyakh D I, Dumitrescu E F, Powers S S and Humble T S 2020 *Quantum Science and Technology* **5** 024002
 - ³² Sun Q, Berkelbach T C, Blunt N S, Booth G H, Guo S, Li Z, Liu J, McClain J D, Sayfutyarova E R, Sharma S *et al.* 2018 *Wiley Interdisciplinary Reviews: Computational Molecular Science* **8** e1340
 - ³³ Matthews D A, Cheng L, Harding M E, Lipparini F, Stopkowicz S, Jagau T C, Szalay P G, Gauss J and Stanton J F 2020 *The Journal of Chemical Physics* **152**
 - ³⁴ Perera A, Bartlett R J, Sanders B A, Lotrich V F and Byrd J N 2020 *The Journal of Chemical Physics* **152**
 - ³⁵ Hehre W J, Stewart R F and Pople J A 1969 *The Journal of Chemical Physics* **51** 2657–2664
 - ³⁶ Grimsley H R, Claudino D, Economou S E, Barnes E and Mayhall N J 2019 *Journal of Chemical Theory and Computation* **16** 1–6
 - ³⁷ Peruzzo A, McClean J, Shadbolt P, Yung M H, Zhou X Q, Love P J, Aspuru-Guzik A and O’Brien J L 2014 *Nature Communications* **5**
 - ³⁸ Taube A G and Bartlett R J 2009 *The Journal of chemical physics* **130**
 - ³⁹ Taube A G and Bartlett R J 2008 *The Journal of Chemical Physics* **128**

Supplementary Material for A new “gold standard”: perturbative triples corrections in unitary coupled cluster theory and prospects for quantum computing*

Zachary W. Windom^{1,2}, Daniel Claudino^{2†}, and Rodney J. Bartlett¹
¹*Quantum Theory Project, University of Florida, Gainesville, FL, 32611, USA*
²*Computational Sciences and Engineering Division, Oak Ridge National Laboratory, Oak Ridge, TN, 37831, USA*

I. SUPPORTING DERIVATIONS OF FINITE-ORDER UCC EQUATIONS

In the case where an ambiguous expression could conceivably have internally disconnected (D) pieces, the overall connected (and necessarily linked) diagram is decomposed into underlying connected (C) and disconnected (D) pieces using

$$\langle 0|XH_NY|0\rangle_C = \frac{1}{2} \left(\langle 0|X(H_NY)_D + X(H_NY)_C + (XH_N)_D Y + (XH_N)_C Y|0\rangle \right) \quad (S1)$$

for X and Y non-vanishing arbitrary strings of T_n and T_n^\dagger operators, and the factor of $\frac{1}{2}$ compensating for overcounting. The internally disconnected (D) pieces can be factored into a connected (C) form via

$$T_n^\dagger \left(H_N T_i T_j \right)_D = T_n^\dagger T_i \left(H_N T_j \right)_C + T_n^\dagger T_j \left(H_N T_i \right)_C \quad (S2)$$

As the following derivations define the UCC energy functional with respect to various MBPT orders, we follow the convention that $\Delta E^{[i]}$ indicates a correction at a particular order, i , all of which can be summed through order n to define the cumulative correction, $\Delta E(n)$:

$$\Delta E(n) = \sum_{i=2}^n \Delta E^{[i]}, \quad (S3)$$

Furthermore, we assume the non-canonical orbitals have been semi-canonicalized such that $f_{ij} = f_{ab} = 0$ for $i \neq j$ and $a \neq b$.

A. Background for deriving the non-canonical HF UCC equations

B. Derivation of UCC(2)

The second order energy functional is of the form

$$\begin{aligned} \Delta E(2) &= \langle 0|\tau_2^\dagger W_N|0\rangle + \langle 0|W_N \tau_2|0\rangle + \langle 0|\tau_2^\dagger f_N \tau_2|0\rangle + \langle 0|\tau_1^\dagger W_N|0\rangle + \langle 0|W_N \tau_1|0\rangle + \langle 0|\tau_1^\dagger f_N \tau_1|0\rangle \\ &= \langle 0|T_2^\dagger W_N|0\rangle + \langle 0|W_N T_2|0\rangle + \langle 0|T_2^\dagger f_N T_2|0\rangle + \langle 0|T_1^\dagger W_N|0\rangle + \langle 0|W_N T_1|0\rangle + \langle 0|T_1^\dagger f_N T_1|0\rangle \end{aligned} \quad (S4)$$

Upon variation of the above with respect to T_2 (or, equivalently, T_2^\dagger) we see that

$$\begin{aligned} \frac{\partial \Delta E(2)}{\partial (t_{ij}^{ab})^\dagger} &= \langle \Phi_{ij}^{ab} | (W_N + f_N T_2) | 0 \rangle \\ &\implies D_2 T_2 = W_N, \end{aligned} \quad (S5)$$

[†] claudinodc@ornl.gov

*This manuscript has been authored by UT-Battelle, LLC, under Contract No. DE-AC0500OR22725 with the U.S. Department of Energy. The United States Government retains and the publisher, by accepting the article for publication, acknowledges that the United States Government retains a non-exclusive, paid-up, irrevocable, world-wide license to publish or reproduce the published form of this manuscript, or allow others to do so, for the United States Government purposes. The Department of Energy will provide public access to these results of federally sponsored research in accordance with the DOE Public Access Plan.

with the last line representing the MBPT(2) residual equations if using canonical HF orbitals. Variation with respect to T_1^\dagger leads to

$$\begin{aligned} \frac{\partial \Delta E(2)}{\partial (t_i^a)^\dagger} &= \langle \Phi_i^a | (f_{ai} + f_N T_1) | 0 \rangle \\ &\implies D_1 T_1 = f_{ai} \end{aligned} \quad (S6)$$

By inserting the residual condition found in Equations S5 and S6 into Equation S4 and further invoking the resolution of the identity - $1 = |0\rangle \langle 0| + |\Phi_{ij}^{ab}\rangle \langle \Phi_{ij}^{ab}|$ - the final energy expression becomes the familiar one from MBPT(2) for general, non-canonical HF references

$$\Delta E(2) = \langle 0 | W_N T_2 | 0 \rangle + \langle 0 | f_{ia} T_1 | 0 \rangle \quad (S7)$$

C. Derivation of UCC(3)

At third-order, we are interested in the functional

$$\begin{aligned} \Delta E^{[3]} &= \left(-\frac{1}{2} \langle 0 | T_2^\dagger T_1 f_N T_1 + \text{h.c.} | 0 \rangle + \frac{1}{2} \langle 0 | (T_1^\dagger)^2 f_N T_2 + \text{h.c.} | 0 \rangle \right) \\ &\quad + \left(-\frac{1}{2} \langle 0 | T_2^\dagger T_1 W_N + \text{h.c.} | 0 \rangle + \frac{1}{2} \langle 0 | (T_1^\dagger)^2 W_N + \text{h.c.} | 0 \rangle \right) \\ &\quad + \langle 0 | (T_1^\dagger + T_2^\dagger) W_N (T_1 + T_2) | 0 \rangle \end{aligned} \quad (S8)$$

We will show that the first two lines in the above completely cancel, leaving the final term to contribute in the UCC(3) energy functional. To show this, we will expand those expressions and group relevant terms such that

$$\begin{aligned} - \left(\langle 0 | T_2^\dagger T_1 f_N T_1 | 0 \rangle + \text{h.c.} \right) &\equiv \langle 0 | T_2^\dagger T_1 W_N | 0 \rangle + \text{h.c.} \\ - \left(\langle 0 | (T_1^\dagger)^2 f_N T_2 | 0 \rangle + \text{h.c.} \right) &\equiv \langle 0 | (T_1^\dagger)^2 W_N | 0 \rangle + \text{h.c.} \end{aligned} \quad (S9)$$

where strict equivalence is found once we arrange the l.h.s. and r.h.s. to emulate the UCC(2) residual equations. This exhausts the viable contractions in the first two terms of Equation S8, leaving only the last term in the energy functional.

Thus, the cumulative functional at third order can be expressed as

$$\begin{aligned} \Delta E(3) &= \underbrace{\langle 0 | (T_1^\dagger + T_2^\dagger) W_N (T_1 + T_2) | 0 \rangle}_{\Delta E^{[3]}} \\ &\quad + \underbrace{\langle 0 | T_2^\dagger W_N | 0 \rangle + \langle 0 | W_N T_2 | 0 \rangle + \langle 0 | T_2^\dagger f_N T_2 | 0 \rangle + \langle 0 | T_1^\dagger W_N | 0 \rangle + \langle 0 | W_N T_1 | 0 \rangle + \langle 0 | T_1^\dagger f_N T_1 | 0 \rangle}_{\Delta E^{[2]}} \end{aligned} \quad (S10)$$

Determining the corresponding set of residual equations requires variation of the above with respect to both T_2/T_2^\dagger and T_1/T_1^\dagger , leading to

$$\begin{aligned} \frac{\partial \Delta E(3)}{\partial (t_{ij}^{ab})^\dagger} &= \langle \Phi_{ij}^{ab} | (W_N + f_N T_2 + W_N T_2 + W_N T_1) | 0 \rangle \\ &\implies D_2 T_2 = W_N + W_N T_2 + W_N T_1 \end{aligned} \quad (S11)$$

which defines the T_2 equations and

$$\begin{aligned} \frac{\partial \Delta E(3)}{\partial (t_i^a)^\dagger} &= \langle \Phi_i^a | (f_{ai} + f_N T_1 + W_N T_1 + W_N T_2 + T_1^\dagger W_N) | 0 \rangle \\ &\implies D_1 T_1 = f_{ai} + W_N T_1 + W_N T_2 \end{aligned} \quad (S12)$$

which defines the T_1 equations.

Following the procedure detailed in UCC(2), we can insert the residual conditions found above into the energy expression of Equation S10 which yields the final expression for the third-order energy

$$\Delta E(3) = \langle 0|W_N T_2|0\rangle + \langle 0|f_{ia} T_1|0\rangle \quad (\text{S13})$$

The set of equations generated by this procedure are the linearized CCSD equations for non-HF examples.

D. Derivation of UCC(4)

Turning to the fourth-order energy functional:

$$\Delta E^{[4]} = \Delta E^{[4A]} + \Delta E^{[4B]} \quad (\text{S14})$$

where

$$\begin{aligned} \Delta E^{[4A]} = & - \langle 0|\frac{1}{3!}\left((T_1^\dagger)^2 T_1 f_N T_1 + \text{h.c.} + (T_2^\dagger)^2 T_2 f_N T_2 + \text{h.c.}\right) + \frac{1}{2}\left(T_3^\dagger T_1 f_N T_2 + \text{h.c.} + T_3^\dagger T_2 f_N T_1 + \text{h.c.}\right)|0\rangle \\ & - \frac{1}{3} \langle 0|T_1^\dagger T_2^\dagger T_1 f_N T_2 + \text{h.c.} + T_2^\dagger T_1^\dagger T_2 f_N T_1 + \text{h.c.}|0\rangle \\ & - \langle 0|\frac{1}{3!}\left((T_1^\dagger)^2 T_1 W_N + \text{h.c.}\right) + \frac{1}{3!}\left((T_2^\dagger)^2 T_2 W_N + \text{h.c.}\right) + \frac{1}{2}\left(T_3^\dagger T_1 W_N + \text{h.c.} + T_3^\dagger T_2 W_N + \text{h.c.}\right)|0\rangle \\ & - \frac{1}{3} \langle 0|T_1^\dagger T_2^\dagger T_1 W_N + \text{h.c.} + T_2^\dagger T_1^\dagger T_2 W_N + \text{h.c.}|0\rangle - \frac{1}{6} \langle 0|T_2^\dagger T_1 T_1^\dagger f_N T_2 + \text{h.c.} + T_2^\dagger T_1 T_1^\dagger W_N + \text{h.c.}|0\rangle \end{aligned} \quad (\text{S15})$$

$$\begin{aligned} \Delta E^{[4B]} = & \frac{1}{4} \langle 0|(T_1^\dagger)^2 f_N T_1^2 + (T_2^\dagger)^2 f_N T_2^2|0\rangle + \langle 0|T_3^\dagger f_N T_3|0\rangle + \langle 0|T_3^\dagger f_N T_1 T_2 + \text{h.c.}|0\rangle + \langle 0|T_1^\dagger T_2^\dagger f_N T_1 T_2|0\rangle \\ & + \frac{1}{2} \langle 0|(T_1^\dagger)^2 W_N T_1 + \text{h.c.} + (T_2^\dagger)^2 W_N T_2 + \text{h.c.}|0\rangle + \langle 0|T_3^\dagger W_N (T_1 + T_2) + \text{h.c.}|0\rangle + \langle 0|T_2^\dagger T_1^\dagger W_N (T_1 + T_2) + \text{h.c.}|0\rangle \\ & - \frac{1}{2} \langle 0|T_2^\dagger T_1 W_N (T_1 + T_2) + \text{h.c.}|0\rangle + \frac{1}{2} \langle 0|(T_1^\dagger)^2 W_N T_2 + \text{h.c.}|0\rangle \end{aligned} \quad (\text{S16})$$

we assign the functional with nomenclature **A** and **B** to denote relevant sections in which there is internal cancellation of disconnected diagrams. We note that the majority of elements that involve f_N and do not linearly coupled with the τ_n^\dagger/τ_n are in need of being canceled.

Starting with **A**, there are seven internal cancellations that are facilitated by invoking the UCC(2) residual equations, causing all terms to cancel

$$\begin{aligned} - \left(T_3^\dagger T_1 f_N T_2 + \text{h.c.} \right) &= T_3^\dagger T_1 W_N + \text{h.c.} \\ - \left(T_3^\dagger T_2 f_N T_1 + \text{h.c.} \right) &= T_3^\dagger T_2 W_N + \text{h.c.} \\ - \left((T_1^\dagger)^2 T_1 f_N T_1 + \text{h.c.} \right) &= (T_1^\dagger)^2 T_1 W_N + \text{h.c.} \\ - \left((T_2^\dagger)^2 T_2 f_N T_2 + \text{h.c.} \right) &= (T_2^\dagger)^2 T_2 W_N + \text{h.c.} \\ - \left(T_1^\dagger T_2^\dagger T_2 f_N T_1 + \text{h.c.} \right) &= T_1^\dagger T_2^\dagger T_2 W_N + \text{h.c.} \\ - \left(T_2^\dagger T_1^\dagger T_1 f_N T_2 + \text{h.c.} \right) &= T_2^\dagger T_1^\dagger T_1 W_N + \text{h.c.} \\ - \left(T_2^\dagger T_1 T_1^\dagger f_N T_2 + \text{h.c.} \right) &= T_2^\dagger T_1 T_1^\dagger W_N + \text{h.c.} \end{aligned} \quad (\text{S17})$$

such that $\Delta E^{[4A]} = 0$. Moving to \mathbf{B} in $\Delta E^{[4B]}$, we invoke Equations S1 and S2 to separate out the internally connected and disconnected pieces of $\Delta E^{[4B]}$:

$$\begin{aligned}
T_3^\dagger(f_N T_1 T_2)_D &= \left(T_3^\dagger T_1 (f_N T_2)_C + T_3^\dagger T_2 (f_N T_1)_C \right) \\
T_1^\dagger T_2^\dagger (f_N T_1 T_2)_D &= T_1^\dagger T_2^\dagger T_2 (f_N T_1)_C + T_1^\dagger T_2^\dagger T_1 (f_N T_2)_C \\
(T_1^\dagger T_2^\dagger W_N T_2)_C &= \frac{1}{2} \left(T_1^\dagger T_2^\dagger (W_N T_2)_D + T_1^\dagger T_2^\dagger (W_N T_2)_C \right) \\
&= \frac{1}{2} \left(T_1^\dagger T_2^\dagger T_2 (W_N)_C + T_1^\dagger T_2^\dagger (W_N T_2)_C \right) \\
(T_3^\dagger W_N T_2)_C &= \frac{1}{2} \left(T_3^\dagger (W_N T_2)_D + T_3^\dagger (W_N T_2)_C \right) \\
&= \frac{1}{2} \left(T_3^\dagger T_2 (W_N)_C + T_3^\dagger (W_N T_2)_C \right)
\end{aligned} \tag{S18}$$

Using these identities, the following internal cancellations arise in $\Delta E^{[4B]}$:

$$- \frac{1}{4} (T_1^\dagger)^2 f_N T_1^2 \equiv \frac{1}{4} \left(T_1^\dagger W_N T_1^2 + \text{h.c.} \right) \tag{S19a}$$

$$- \frac{1}{4} (T_2^\dagger)^2 f_N T_2^2 \equiv \frac{1}{4} \left(T_2^\dagger W_N T_2^2 + \text{h.c.} \right) \tag{S19b}$$

$$- T_1^\dagger T_2^\dagger T_2 f_N T_1 = T_1^\dagger T_2^\dagger W_N T_2 + \text{h.c.} \tag{S19c}$$

$$- T_1^\dagger T_2^\dagger T_1 f_N T_2 = T_1^\dagger T_2^\dagger W_N T_1 + \text{h.c.} \tag{S19d}$$

$$- T_3^\dagger T_2 f_N T_1 + \text{h.c.} = T_3^\dagger T_2 W_N + \text{h.c.} \tag{S19e}$$

$$- T_3^\dagger T_1 f_N T_2 + \text{h.c.} = T_3^\dagger T_1 W_N + \text{h.c.} \tag{S19f}$$

$$- \left(T_2^\dagger T_1 f_N T_1 + \text{h.c.} \right) = \left(T_2^\dagger T_1 W_N + \text{h.c.} \right) + \left(T_2^\dagger T_1 W_N T_1 + \text{h.c.} \right) + \left(T_2^\dagger T_1 W_N T_2 + \text{h.c.} \right) \tag{S19g}$$

$$- \left((T_1^\dagger)^2 f_N T_2 + \text{h.c.} \right) = \left((T_1^\dagger)^2 W_N + \text{h.c.} \right) + \left((T_1^\dagger)^2 W_N T_1 + \text{h.c.} \right) + \left((T_1^\dagger)^2 W_N T_2 + \text{h.c.} \right) \tag{S19h}$$

Equations S19a and S19b cancel incompletely, leaving $\frac{1}{4} \left((T_1^\dagger W_N T_1^2 + \text{h.c.}) + T_2^\dagger W_N T_2^2 + \text{h.c.} \right)$ in the UCC(4) functional. The identities of Equation S18 are used to invoke the cancellations found in Equations S19c-S19f, noting that the connected portions of $\left(T_1^\dagger T_2^\dagger (W_N T_2)_C + \text{h.c.} \right)$ and $\left(T_3^\dagger W_N T_2 + \text{h.c.} \right)$ survive in the UCC(4) functional. Finally, note that Equations S19g and S19h invoke the UCC(3) T_1 and T_2 residual equations, respectively, to instigate cancellation in the UCC(4) functional by taking advantage of Equation S9.

These simplifications lead to a significantly reduced expression for the UCC(4) energy functional:

$$\begin{aligned}
\Delta E^{[4]} &= \langle 0 | T_3^\dagger f_N T_3 | 0 \rangle + \frac{1}{4} \left(\langle 0 | T_1^\dagger W_N T_1^2 | 0 \rangle + \text{h.c.} \right) + \frac{1}{4} \left(\langle 0 | T_2^\dagger W_N T_2^2 | 0 \rangle + \text{h.c.} \right) \\
&\quad + \langle 0 | T_3^\dagger W_N T_2 | 0 \rangle + \langle 0 | T_2^\dagger W_N T_3 | 0 \rangle + \langle 0 | T_2^\dagger T_1^\dagger W_N T_2 + T_2^\dagger W_N T_1 T_2 | 0 \rangle
\end{aligned} \tag{S20}$$

Taking the partial derivative of the full $\Delta E(4) \equiv \Delta E^{[2]} + E^{[3]} + E^{[4]}$ functional yields the corresponding set of residual equations for UCC(4)

$$\begin{aligned}
D_1 T_1 &= W_N + W_N T_2 + W_N T_1 + \frac{1}{2} \left(\frac{1}{2} W_N T_1^2 + T_1^\dagger W_N T_1 \right) + T_2^\dagger W_N T_2 \\
D_2 T_2 &= W_N + W_N T_2 + W_N T_1 + \frac{1}{2} \left(\frac{1}{2} W_N T_2^2 + T_2^\dagger W_N T_2 \right) + W_N T_3 + T_1^\dagger W_N T_2 + W_N T_1 T_2 \\
D_3 T_3 &= W_N T_2
\end{aligned} \tag{S21}$$

Inserting these residual equations back into the energy functional of Equation S20, we find the final UCC(4) energy can be expressed as

$$\Delta E(4) = \langle 0|W_N T_2|0\rangle + \langle 0|W_N T_1|0\rangle - \frac{1}{4} \left(\langle 0|(T_1^\dagger)^2 W_N T_1|0\rangle + \langle 0|(T_2^\dagger)^2 W_N T_2|0\rangle \right) \quad (\text{S22})$$

II. MOLECULAR GEOMETRIES

Molecule	State	r (Å)
H ₂ O	¹ Σ	0.95785
CO	¹ Σ	1.128
C ₂	¹ Σ	1.243
O ₂	¹ Δ _g	1.2075
N ₂	¹ Σ	1.098

TABLE S1: Geometry of molecules studied in this work. H₂O has internal angle of 104.5°. Information taken from Ref. 1

III. MOLECULAR ENERGIES

Method	H ₂ O	CO	C ₂	O ₂	N ₂
FCI	-75.7287768	-112.4426091	-75.4339744	-149.1251956	-108.7003854
UCCSD	-75.7286759	-112.4344259	-75.4220734	-149.1160634	-108.6982094
UCCSD[T]	-75.7287535	-112.4365040	-75.4388158	-149.1191769	-108.7000018
UCCSD(T)	-75.7287624	-112.4366356	-75.4422217	-149.1192170	-108.7000296
UCCSD(T*)	-75.7287535	-112.4365384	-75.4409788	-149.1191937	-108.7000143
tUCCSD	-75.7286780	-112.4347203	-75.4228943	-149.1160736	-108.6982132
tUCCSD[T]	-75.7287561	-112.4443853	-75.4400836	-149.1193527	-108.6997618
tUCCSD(T)	-75.7287645	-112.4456299	-75.4439410	-149.1193946	-108.6997886
tUCCSD(T*)	-75.7287560	-112.4447561	-75.4425394	-149.1193699	-108.6997732

TABLE S2: Molecular energies reported in this work.

IV. EFFECT OF OPERATOR ORDERING

Here we provide numerical evidence for the claim that the operator ordering has a sizable effect in the energetics as the N₂ departs from the equilibrium region. First, we simply follow the strategy laid out in the main text, we end up Figures S1 and S2, where we see that tUCCSD and the corresponding [T] do not yield smooth curves, while UCCSD and UCCSD[T] do.

We further analyze this by focusing on energies at $r = 2.5$ Å. For this we report energies with the ordering described in Equation in the main text, its reverse order, and 10 orderings obtained randomly, assigned number 1-10 (these numbers have no particular meaning). The corresponding energies are reported in Table S3, on which we only included excitations whose CCSD amplitudes had absolute value above 10^{-12} .

A similar trend persists even if no information is taken from CCSD, which is faulty in this region, as shown in Table S4.

When we use the ordering shown in Equation in the main text, we can perform two simple comparisons involving the Frobenius norm of the amplitudes along the potential energy surfaces, further displaying the effect of the operator ordering in tUCCSD. We plot those in Figure S3.

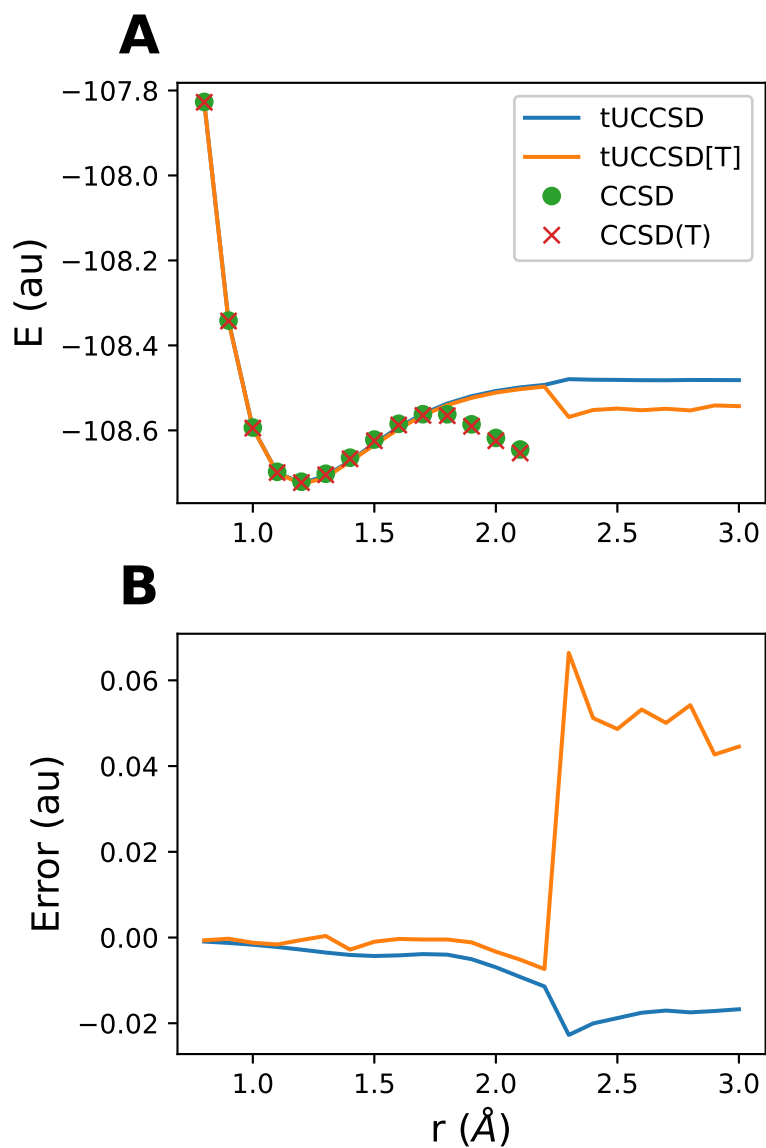


FIG. S1: Comparison of the trotterized UCCSD operator and its perturbative, triples correction against their classical CC analogs for the dissociation of the N₂ dimer.

¹ Johnson, R. Computational Chemistry Comparison and Benchmark Database, NIST Standard Reference Database 101. (National Institute of Standards, 2002), <http://cccbdb.nist.gov/>

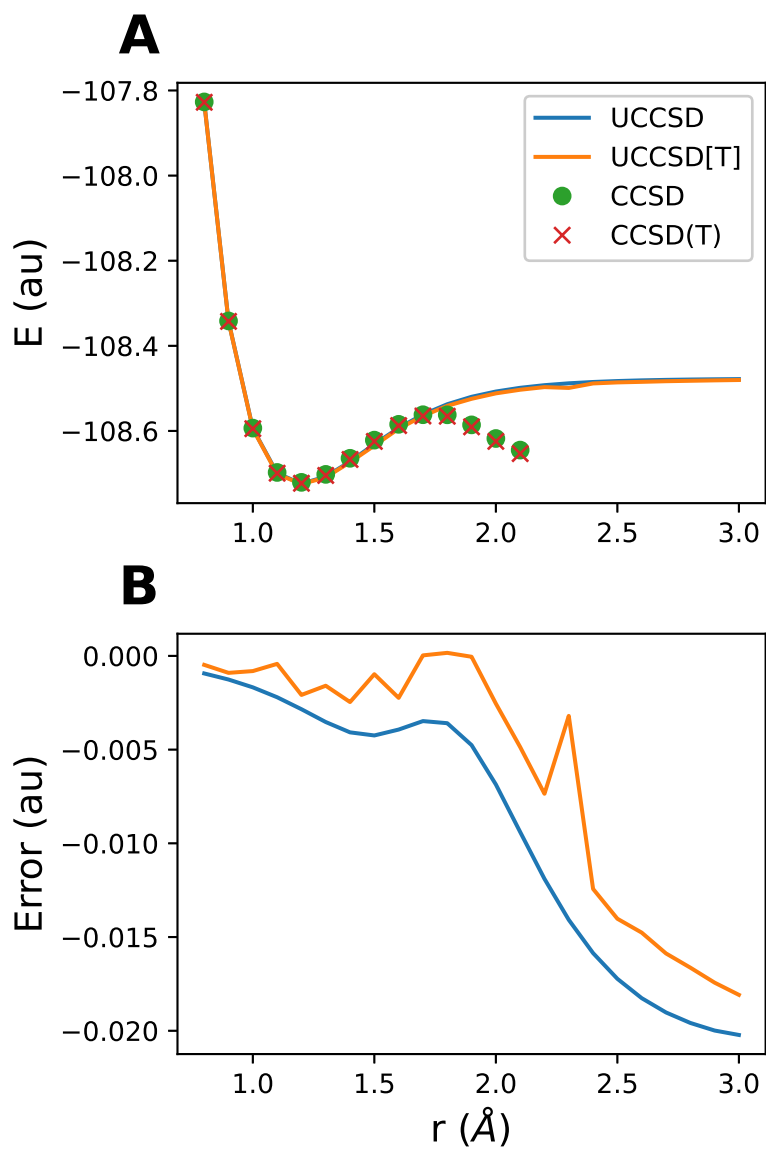


FIG. S2: Comparison of the full UCCSD operator and its perturbative, triples correction against their classical CC analogs for the dissociation of the N_2 dimer.

Ordering	tUCCSD	error (mH)	tUCCSD[T]	error (mH)
Original	-108.4811739	-18.7954623	-108.5486183	48.6489742
Reverse	-108.4852511	-14.7182743	-108.4937380	-6.2313152
1	-108.4791585	-20.8108577	-108.4864910	-13.4783461
2	-108.4788495	-21.1198423	-108.4836705	-16.2987984
3	-108.481179	-18.7903034	-108.4885425	-11.4268748
4	-108.4731937	-26.7756670	-108.4807869	-19.1824444
5	-108.4738939	-26.0753895	-108.4819188	-18.0505767
6	-108.4705049	-29.4643874	-108.4825742	-17.3951401
7	-108.4816735	-18.2958133	-108.4904421	-9.5272657
8	-108.4749829	-24.9864422	-108.4832488	-16.7205052
9	-108.4827561	-17.2132415	-108.4901482	-9.8211059
10	-108.4764604	-23.5089757	-108.4850187	-14.9506337

TABLE S3: Assessing the impact of operator ordering on the sensitivity of the tUCCSD/[T] result for the N₂ molecule at $r = 2.5$ Å. "Original" is the original ordering specified in the manuscript - that depends on the underlying CCSD amplitudes - and "Reverse" is the reverse ordering. Shuffles 1-10 are ordered at random. These results are with respect to an CCSD amplitudes being used as an initial guess to the UCCSD amplitudes.

Shuffle	tUCCSD	error (mH)	tUCCSD[T]	error (mH)
1	-108.4762272	-23.7421647	-108.4817067	-18.2626184
2	-108.4800833	-19.8860206	-108.4931779	-6.7914257
3	-108.4842005	-15.7687809	-108.4967363	-3.2330415
4	-108.4757842	-24.1851546	-108.4887858	-11.1834957
5	-108.4770212	-22.9481237	-108.4884296	-11.5396819
6	-108.479732	-20.2373132	-108.4915446	-8.4247227
7	-108.4834032	-16.5661744	-108.4951588	-4.8105400
8	-108.4717318	-28.2375010	-108.4832757	-16.6936299
9	-108.4781734	-21.7959566	-108.4825076	-17.4617319
10	-108.4763993	-23.5699863	-108.4917173	-8.2520276

TABLE S4: Assessing the impact of operator ordering on the sensitivity of the tUCCSD/[T] result for the N₂ molecule at $r = 2.5$ Å. Shuffles 1-10 are ordered at random. These results are with respect to no initial guess for the UCCSD tau amplitudes.

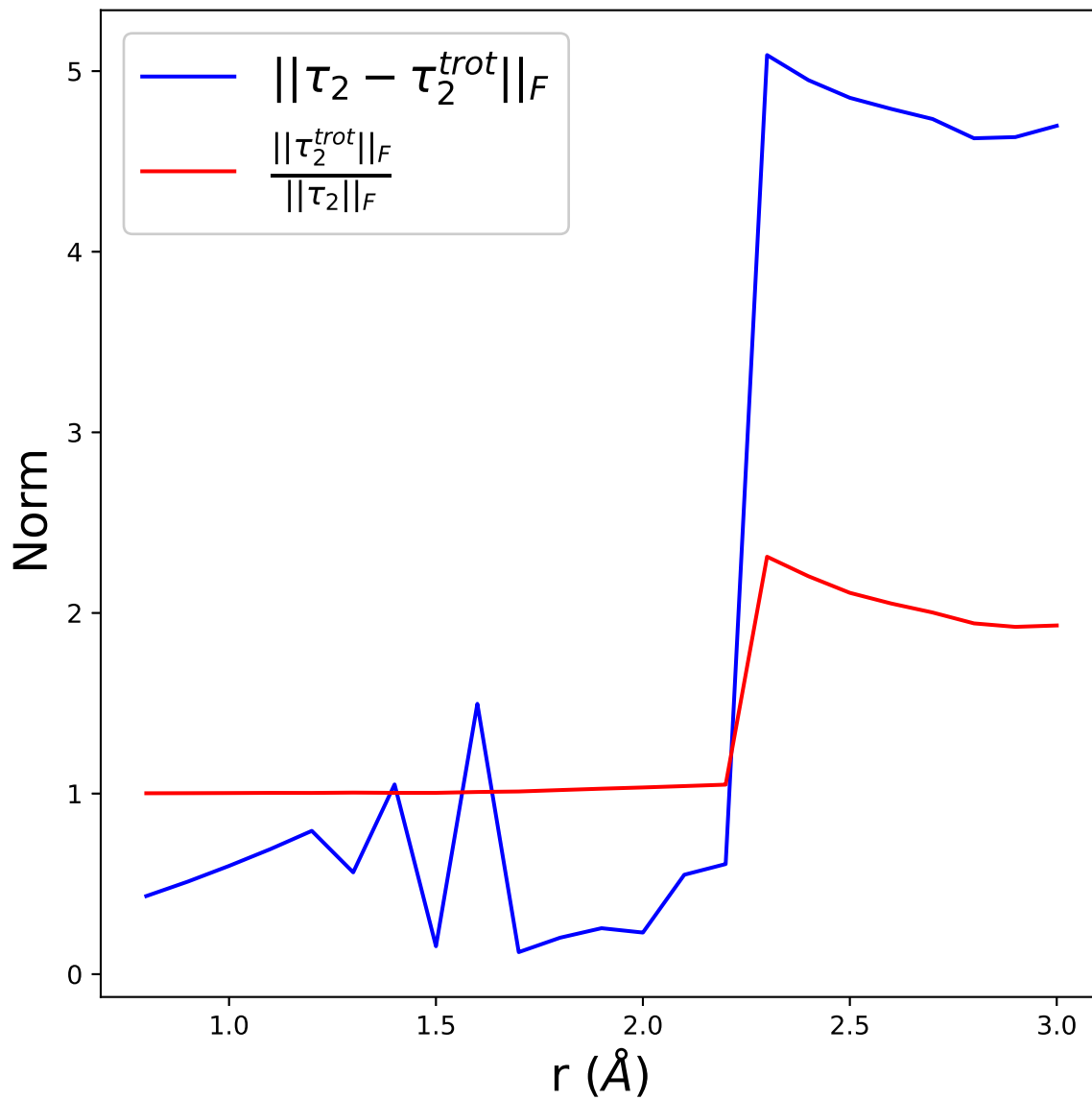


FIG. S3: Frobenius norm comparison of the tUCCSD operator and the corresponding full operator along the potential energy surface for N_2 . τ_2 signifies the full operator, whereas τ_2^{trot} specifies the Trotterized variant.